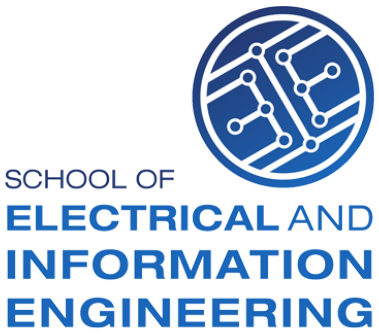

Laboratory Assignment

Bionic Finger Force Measurement System

ELEN4006

School of Electrical & Information Engineering, University of the Witwatersrand, Private Bag 3, 2050, Johannesburg, South Africa

Aidan Rabinowitz (2341197), Joshua Schwark (2118091)

Submission Date: 20th May 2024

Abstract: A measurement system is designed to enable finger sensory force feedback for patients using a bionic hand. The FSR402 Force Sensitive Resistor is the sensing element for input force. The output of this sensor is conditioned with a voltage divider and a buffer, and processed with a low-pass filter and microcontroller, to convert input force into output voltage, which is linearised and scaled using a mathematical formula, to display the input force. The system output is 98% accurate from 0 N to 10 N and has a maximum error of 28.4 % at higher force input, when compared to known reference forces. This error is attributed to lowered resolution at higher force input. The group worked efficiently and timeously to ensure all phases of the project were completed.

1 Introduction

Individuals using bionic hands may lack sensory feedback when grabbing items, which causes grip-strength misinterpretation[1, 2]. This report entails the design, construction, testing methodology and performance review of a measurement system to detect force applied to a Force Sensitive Resistor (FSR) on the tip of the index finger of a bionic hand, and display the force. The assignment focuses on developing skills for recording and analysing measurement data as part of the design process. The report covers the system design specifications, high-level solution and detailed design. System performance is evaluated through testing at each stage, and a critical analysis regarding design specification adherence is performed.

2 Design Specification and High-level Solution

The FSR resistance decreases as force is applied to it. A voltage divider is created by applying 3.3V to the FSR in series with a resistor to obtain a voltage output signal, which leads to a buffer op-amp to reduce loading effects. From this, the signal is processed using a low-pass filter, seen in Figure 1, which attenuates switch-bouncing noise[3]. The system is designed according to the specifications in Table 1, for a patient requiring finger force sensory feedback. The actual measured signal ranges are in Table 1.

Table 1: Design Specifications

PARAMETER	**VALUE**	**NOTES**
Force Sensitivity	>0.1V/N	Required for grabbing items[4]
IP Rating	IP 65	Protected from water damage
Turn-on Force	0.1N	At least record 0.1N
Stand-Off Resistance	> 1 MΩ	0N resistance
Device Rise Time	<35ms	For fine motor response[5]
Bandwidth	> 10Hz	Based on finger muscle action potential time [6]
Temperature Range	-10 ºC to 40 ºC	Edge-case likely operating temperature
Accuracy	10%	Avoid object dropping or breakage
Sensitivity with Noise and Vibration	5% Error	Button/Switching Noise[3]
Force-sensitive Range	0.3 N-30 N	Allowing a wide range of force feedback

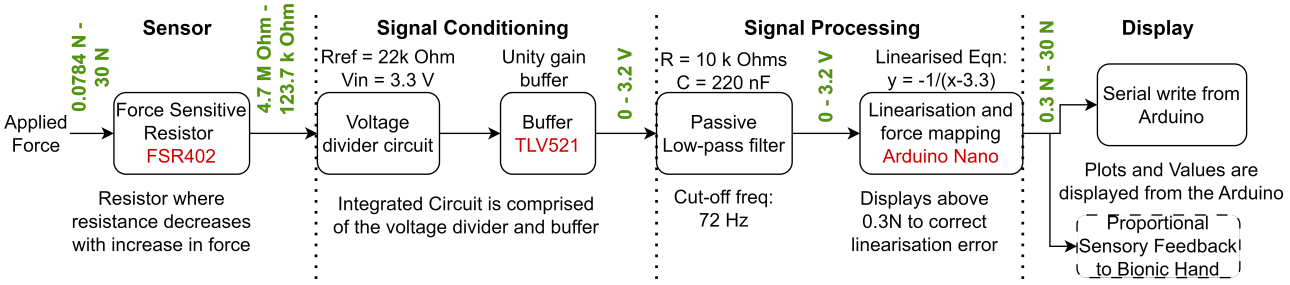

Figure 1: High-Level Diagram of the System

3 Detailed Design

The high-level design and justifications for design choices are explained below:

Sensor: The FSR402 is used [7], as it agrees with the system design specifications and is affordable. The datasheet states that the FSR rise time is less than 3 µs[7], which infers a -3dB bandwidth of 11 kHz, assuming a 1st order system [8, 9]. However, a bandwidth of 3500 Hz is measured, calculated from the rise time from the step response[9] in Figure 6. The force-sensitive range is equal to the design specification.

Signal Conditioning: An integrated circuit (IC) is used, containing a voltage divider with a 22KR_{div} resistor and a TLV521 op-amp for force-to-voltage conversion defined by equation 1:

$$V_o = V_i \cdot \frac{R_{\text{div}}}{R_{\text{fsr}} + R_{\text{div}}} \tag{1}$$

Applying a force to the FSR causes a visible hyperbolic decrease in resistance and reflected increase in voltage, as in Figure 3, lowering resolution and sensitivity as force is increased. Lower R_{div} increases overall sensitivity but the IC used presents ample sensitivity, with experiments showing no improvement with lower R_{ref} values above 10N input force. The TLV521 has a high input impedance and gain-bandwidth product, with low voltage drift and offset, minimising error[10]. The output voltage range in Figure 1 does not reach the 3.3V input because this also supplies the op-amp rails.

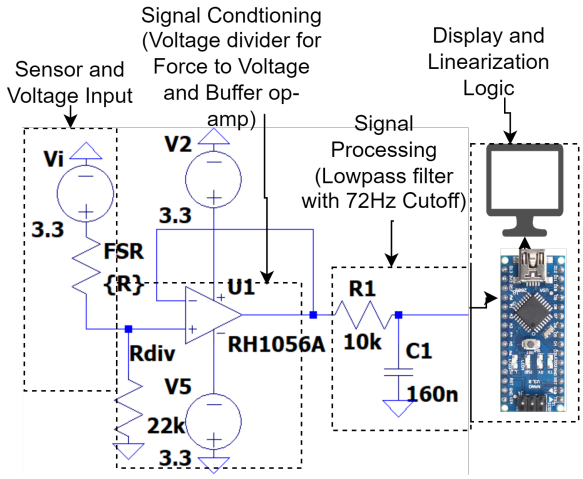

Figure 2: Circuit Diagram of the FSR Measurement System

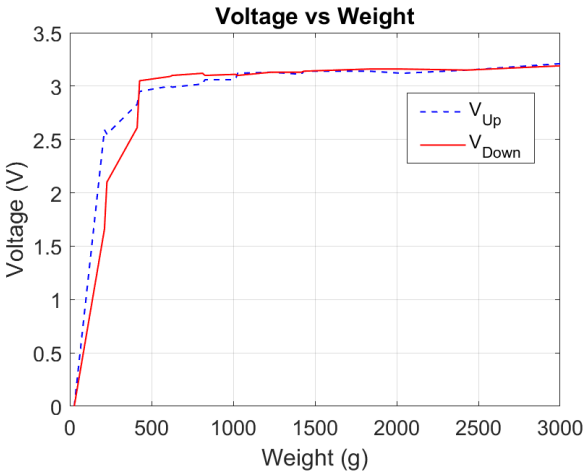

Figure 3: Voltage Hysteresis

Signal Processing: High-frequency noise is prevalent in the system steady-state output signal, forming visible ripples. This is due to switching noise from shaking or electromagnetic interference from hand-held devices [3, 11]. A passive RC low-pass filter, with a -3dB cutoff

frequency designed at 72Hz, but measured at 69Hz, due to component tolerance of +-1%, visibly lowers the steady-state ripple. This leaves the desirable 30Hz bandwidth unaffected and attenuates noise. Signal processing also includes linearisation using the parabolic force-conductance relationship from the FSR. Linearisation improves the ease of integrating the data into a medical device because of the intuitive input-output relationship. Applying force to the FSR causes a change in output voltage, ranging from 0 with no force, to Vin (3.3 V) with 30 N of force. This occurs by increasing FSR conductance. Linearisation logic stems from the $F \propto 1/R_{FSR}$ hyperbolic relationship. This logic, seen in Figure 4 is implemented in Arduino code. An Arduino Nano is used because of its small form and sufficiently high ADC conversion speed of 9615 Hz with 10-bit resolution [12]. All relevant circuitry is displayed in Figure 2.

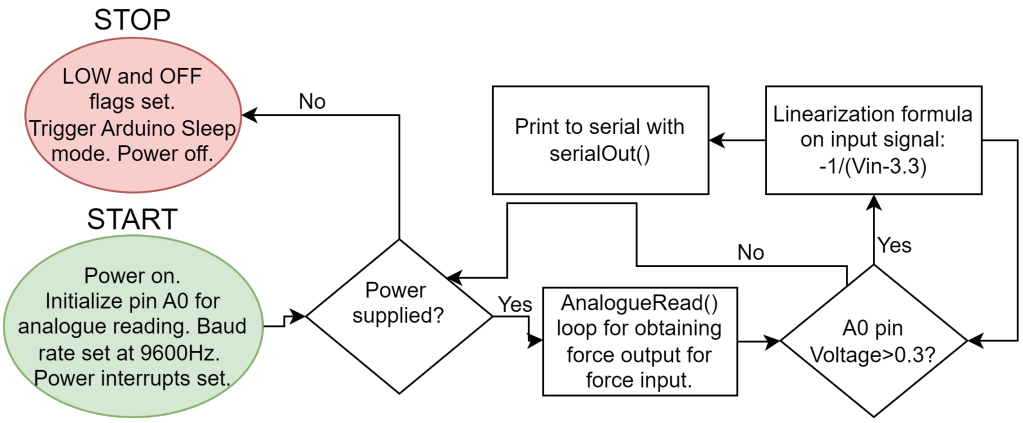

Figure 4: Microprocessor Logic

Display: The system's display is a laptop screen that displays values from the Arduino IDE's serial print function. This display is cheap and efficient for testing, and can be integrated for relevant prostheses, outside the scope of this report, which can include a sensory feedback mechanism to the patient with a vibratory motor.

4 Performance Evaluation

Measurements at each stage from Figure 1 are taken in isolation after a 10 second stabilisation period, with known constant forces in the form of static weights. The measured ranges of these variables are in Figure 1. The bandwidth at each stage after the FSR in Table 2 is measured by obtaining the -3dB point from a frequency sweep. The FSR bandwidth is determined by taking $0.35/T_R$, after measuring the rise time T_R as 1.075ms.

In Table 2, the bandwidth and error of each stage are shown, with the smallest bandwidth limiting system bandwidth, and error propagating additively, as each stage is connected in series. Maximum output error is measured by comparing the additive stage error, and the

maximum linearity error at the system output, against an ideal linear force output in 5. The non-linearity of the system is taken as

$$\frac{(V_{linearized} - V_{ideal})}{V_{idealmax}}, \tag{2}$$

found to be 28.4% at maximum, at 23.86N input force, as in Figure 5, but from 0N to 10N input force, the system output is linear within 2%. Maximum hysteresis error of +22% occurs near 2N input force for the FSR, expected due to its high sensitivity at low force. Loading effects are prevalent at low force input, due to the high resistance of the FSR. These are mitigated via the high input impedance of the TLV521 op-amp, which also minimally increases error with its relatively negligent temperature drift and offset voltage. Beginning system output after 0.3N signal into the Arduino code also lowers the FSR loading, because although a tiny force is required to begin measurement, this makes the initial FSR resistance lower than the maximum 10 MΩ. Figure 6 shows the step-response of the conditioned signal, gathered at 1000 recordings/s in MATLAB. This illustrates the rise time and the system reaching Vin (3.3 V).

Table 2: System Stages with Bandwidth and Error

Stage	**Bandwidth (Hz)**	**Error (%)**	**Error Method**
Measurement (FSR)	3500	2 (0N-10N); 25 (10N-30N)	Hysteresis and Resolution
Conditioning	30	1	Voltage drift & offset
Processing	69	2	Component Tolerances
Display	10000	0.1	Arduino Sampling
TOTAL:	**30**	**28.1**	Additive Error

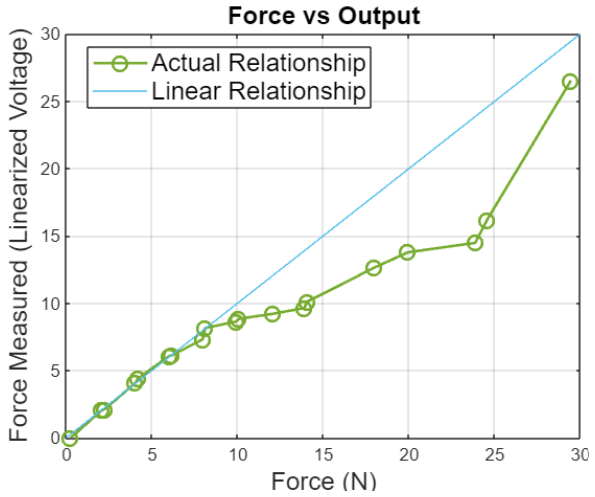

Figure 5: Linearised Force Output & Ideal Force Output

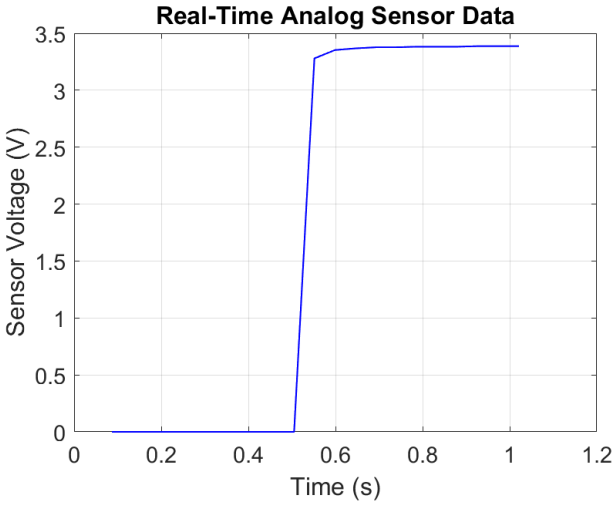

Figure 6: Step Response

5 Critical Analysis

The system fails the error specification for above 10N input force and meets all others. Due to its hysteresis error and varying sensitivity, the FSR is responsible for approximately 89% of the maximum system error. Accurate measurements from the sensor are difficult to obtain because only a small portion of the sensor surface area provides repeatable results, so at least three repetitions of each reading were taken. Figure 5 shows that the sensor is highly accurate between 0 N and 10 N, and may present feedback issues above this input force. The system's bandwidth is limited at 30 Hz due to its conditioning components. This is sufficient, as a human does not require a higher bandwidth than 10 Hz for adequate finger movement [6]. Thus this measurement system is suitable for finger force feedback for a bionic hand for small force input, which enables grabbing of light objects [13, 14]. The system circuitry is designed with simplicity, affordability and efficiency in mind. Few components are used, leaving few points of breakage and improving the ease of system diagnosis. Component costing of R332,40 can lead to competitive pricing against competitors like Galileo [15, 16]. This has a positive ethical effect, through a teleological lens, as it improves accessibility to a wider target market who cannot afford competitor products.

6 Reflection of Group Work

The group worked well together throughout the laboratory project, with both members meeting regularly to discuss progress, allowing for specific milestones to be assessed throughout the semester with the three main milestones being measurements, output scaling and display. The group aimed to complete the report three days before the submission deadline to allow for ample proof-reading and editing to ensure flow between both members writing. The work was distributed equally, with practical measurements done together and research separately, based on individual interest in research topics.

7 Summary and Conclusions

The system meets the design specifications sufficiently, below 10 N input force, and is inaccurate above 10 N. The rise-time is fast enough for a patient to receive appropriate feedback for fine motor tasks. System errors are present above 10N largely due to hyperbolic decreasing of resolution, along with hysteresis. The system output is 98% accurate between 0 N - 10 N and at a maximum, 28.4% erroneous at higher force inputs. The measured results are evaluated against the design specifications for each design section. The group demonstrated effective teamwork and planning throughout the length of the project.

References

[1] M. E. Charness, M. H. Ross, and J. M. Shefner, "Ulnar neuropathy and dystonic flexion of the fourth and fifth digits: clinical correlation in musicians," *Muscle & Nerve: Official Journal of the American Association of Electrodiagnostic Medicine*, vol. 19, no. 4, pp. 431–437, 1996.

[2] U. Wijk, I. K. Carlsson, C. Antfolk, A. Björkman, and B. Rosén, "Sensory Feedback in Hand Prostheses: A Prospective Study of Everyday Use," *Frontiers in Neuroscience*, vol. 14, 2020. Publisher: Frontiers Media SA.

[3] H. Kim, S.-G. Kim, J.-G. Yook, *et al.*, "A localized enhanced power plane topology for wideband suppression of simultaneous switching noise," *IEEE Transactions on Electromagnetic Compatibility*, vol. 52, no. 2, pp. 373–380, 2010.

[4] X.-D. Pang, H. Z. Tan, and N. I. Durlach, "Manual discrimination of force using active finger motion," *Perception & psychophysics*, vol. 49, no. 6, pp. 531–540, 1991.

[5] A. N. Carlsen, R. Chua, J. T. Inglis, D. J. Sanderson, and I. M. Franks, "Differential effects of startle on reaction time for finger and arm movements," *Journal of neurophysiology*, vol. 101, no. 1, pp. 306–314, 2009.

[6] S. C. Salvage, A. P. Jackson, and C. L.-H. Huang, "Structure and function of skeletal muscle," 2020.

[7] I. Electronics, "FSR 402 Data Sheet." Online, Year.

[8] G. Fedele, "A new method to estimate a first-order plus time delay model from step response," *Journal of the Franklin Institute*, vol. 346, no. 1, pp. 1–9, 2009.

[9] D. Weller, "Relating wideband dso rise time to bandwidth: Lose the 0.35!," *EDN*, vol. 47, no. 27, pp. 89–92, 2002.

[10] Texas Instruments, *TLV521 NanoPower, 350nA, RRIO, CMOS Input, Operational Amplifier*, 2023. Accessed: 2024-05-18.

[11] M. J. Sorri, P. J. Piiparinen, K. H. Huttunen, and M. J. Haho, "Solutions to electromagnetic interference problems between cochlear implants and gsm phones," *IEEE Transactions on neural systems and rehabilitation engineering*, vol. 14, no. 1, pp. 101–108, 2006.

[12] "Nano | Arduino Documentation."

[13] V. G. Macefield and R. S. Johansson, "Control of grip force during restraint of an object held between finger and thumb: responses of muscle and joint afferents from the digits," *Experimental brain research*, vol. 108, pp. 172–184, 1996.

[14] C. Winstein, J. Abbs, and D. Petashnick, "Influences of object weight and instruction on grip force adjustments," *Experimental brain research*, vol. 87, pp. 465–469, 1991.

[15] J. Fajardo, V. Ferman, D. Cardona, G. Maldonado, A. Lemus, and E. Rohmer, "Galileo hand: An anthropomorphic and affordable upper-limb prosthesis," *IEEE access*, vol. 8, pp. 81365–81377, 2020.

[16] "Seeed Studio Grove - Round Force Sensor Module for FSR402 | RS."